

# ORBIT PRECISION ANALYSIS OF SMALL MAN-MADE SPACE OBJECTS IN LEO BASED ON RADAR TRACKING MEASUREMENTS

M. Kirschner<sup>(1)</sup>, M. Weigel<sup>(1)</sup>, R. Kahle<sup>(1)</sup>, E. Kahr<sup>(2)</sup>, P. Choi<sup>(3)</sup>, K. Letsch<sup>(4)</sup> and  
L. Leushacke<sup>(4)</sup>

<sup>(1)</sup>German Aerospace Center (DLR), German Space Operations Center(GSOC),  
82234 Wessling, Germany, +49 8153-28-1385, [michael.kirschner@dlr.de](mailto:michael.kirschner@dlr.de)

<sup>(2)</sup>Department of Geomatics Engineering, Schulich School of Engineering, University of Calgary,  
Canada, [erinkahr@hotmail.com](mailto:erinkahr@hotmail.com)

<sup>(3)</sup>Space Flight Laboratory, University of Toronto, Institute for Aerospace Studies,  
4925 Dufferin Street, Toronto, Ontario, Canada, M3H 5T6, [pchoi@utias-sfl.net](mailto:pchoi@utias-sfl.net)

<sup>(4)</sup>Fraunhofer Institute for High Frequency Physics and Radar Techniques (FHR),  
Neuenahrer Str. 20, 53343 Wachtberg, Germany,  
+49 228 9435-343, [klemens.letsch@fhr.fraunhofer.de](mailto:klemens.letsch@fhr.fraunhofer.de)

## **Abstract:**

*The German Space Operations Center (GSOC) performs collision avoidance for 11 LEO and 2 GEO satellites. Risk detection and maneuver decisions strongly depend on the computed probability of collision that is driven by the anticipated orbit precision of chaser and target. While the orbits of operational satellite are well known this is usually not the case for space debris. Therefore, an improved collision assessment requires refined orbit determination of the chaser object.*

*This paper describes the achievable orbit precision for a small object based on radar measurements. The Tracking and Imaging Radar (TIRA) of Fraunhofer FHR in Wachtberg, Germany, was used to track the Canadian nanosatellite CanX-2 over a period of five days. CanX-2 is a triple CubeSat of the size 10x10x34 cm carrying a dual frequency GPS receiver. A reference trajectory is established by precise orbit determination (POD) from GPS measurements. Radar tracking measurements and derived orbital information are evaluated by comparison against the reference orbit. Statistics of the orbit determination and orbit prediction precision using different radar measurement data arc lengths is presented leading to a better understanding of the prediction uncertainty of critical close approaches between an active satellite and a small object.*

**Keywords:** orbit precision, radar tracking, space debris

## **1 Introduction**

The growing number of space objects in the region near the Earth causes more and more concerns about the safety of LEO space missions. The so-called Kessler syndrome describes a scenario where the density of objects in LEO is high enough to induce a cascade of collisions between these objects. After the collision between Iridium 33 and Cosmos 2251 in 2009, many experts consider the cascade as started, implying that the usability of the LEO region could be lost within the next 20 years. These future prospects could be avoided if at least five big pieces of space debris are removed per year beginning in the near future. Besides the active removal of space debris, collision mitigation strategies have to be applied for active satellite missions.

The German Space Operations Center (GSOC) has been implementing a collision avoidance system since 2008 [1], [2]. Bi-daily automated conjunction monitoring is carried out based on the USSTRATCOM catalogue of Two Line Elements (TLE), but the decisions on collision avoidance maneuvers are only based on the Conjunction Summary Messages (CSM) released by the Joint Space Operations Centre (JSpOC) in USA [3], [4]. Although JSpOC has direct access to the tracking data of the Space Surveillance Network (SSN), not all space objects are tracked with the

same frequency and precision. Information about a critical close approach can sometimes have a degraded precision, particularly when combined with the lack of knowledge about the performed or planned maneuvers of an active satellite.

The safe approach and rendezvous, in the case of debris removal, or the reliable estimation of the collision risk, in the case of a critical close approach, both require the orbit of the space debris to be known as precisely as possible. The precise estimation of the orbital elements of the space debris object, or a refinement with respect to the publicly available TLE catalogue, can be achieved using measurements from a dedicated radar tracking campaign.

This study investigates the precision with which the orbit of a small object can be determined and propagated based on radar tracking measurements. The Tracking and Imaging Radar (TIRA) of Fraunhofer FHR in Wachtberg, Germany, was used to track the Canadian nanosatellite CanX-2 over a period of five days. The first part of the paper discusses the orbit of the CubeSat CanX-2 and the timeline of the radar tracking and GPS operations during the 5-days campaign.

Next, the calculation and validation of the reference trajectory is discussed. Precise orbit determination (POD) is performed based on dual frequency GPS carrier phase and pseudorange measurements. The degraded POD accuracy for the periods outside GPS receiver operations is quantified by means of a similar analysis with TerraSAR-X precise orbits. The estimated accuracy of the CanX-2 reference orbit is below the one meter level and below the ten meter level during the GPS outages of up to 36 hours.

Furthermore, the statistics of the achievable orbit determination precision using different radar tracking measurement data arc lengths are presented. The accuracy of an orbit prediction over a period of up to 3 days is analyzed as well. In both cases, orbit determination and propagation, the orbit ephemeris is compared with the POD reference trajectory. For example, for radar tracking scenarios comprising of 6 station passes within a 36 hour period, a remarkable orbit determination accuracy of 10 m in the radial direction (1D, RMS), 100 m (RMS) in the along-track direction and an accuracy of less than 15 m (RMS) in the cross-track direction is computed from comparison to the reference orbit. After 3 days of orbit propagation a corresponding maximum position error of only 170 m (3D, RMS) is found. Of course, both orbit determination and propagation accuracies are significantly degraded in case of shorter observation arcs and less tracking passes.

Finally, subsets of the radar tracking data are selected that cover a limited observation time and limited number of station passes. Multiple tracking scenarios with identical characteristic can be constructed. Mean position errors are computed for groups of identical tracking cases. Thereby, orbit precision is evaluated on a statistical basis, exceeding the analysis of individual cases.

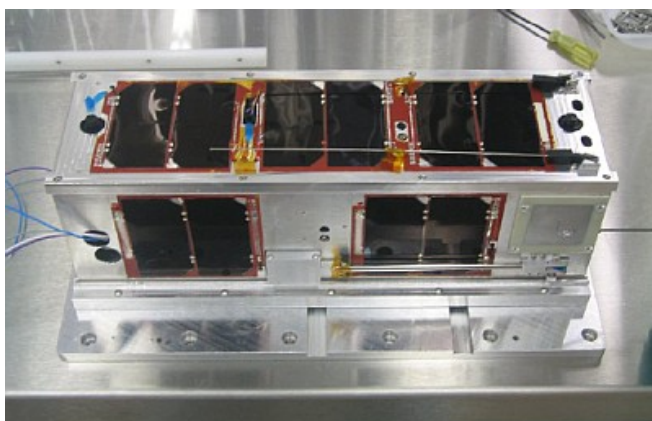


**Figure 1. UTIAS/SFL CanX-2 (left), FHR Tracking and Imaging Radar (right)**

The outcome of this paper is a better understanding of the prediction uncertainty of a critical close approach between an active satellite and a small object, as well as an understanding of the necessary effort required to refine the orbit of a space debris object for safe space debris removal.

## 2. The CanX-2 Measurement Campaign

CanX-2 is a triple CubeSat with dimensions 10 x 10 x 34 cm. It was built under the Canadian Advanced Nanospace eXperiment (CanX) program and is operated by the University of Toronto Institute for Aerospace Studies, Space Flight Laboratory (UTIAS/SFL) [5], [6], [7] and [8]. CanX-2 was launched in April 2008 and is orbiting the Earth in a Sun-synchronous polar orbit with a 635km altitude and a 9:30 am descending node. Although CanX-2 has a cold gas propulsion subsystem capable of affecting small changes to its orbital dynamics, the subsystem was not activated throughout the campaign and, thereby, orbit manoeuvres were not taken into account. Due to the nanosatellite's power, data storage volume and downlink downlink constraints the GPS receiver was only operated for approximately 90 minutes twice daily. The GPS on-time was coordinated with the visibility of CanX-2 for TIRA. Timely synchronization or even simultaneity of observations ensures radar measurement evaluation at times of most precise GPS position information.

The Tracking and Imaging Radar (TIRA) consists of a 34-meter parabolic antenna system with a narrowband, fully coherent mono-pulse tracking radar at L-band (1.333 GHz) as well as a wideband Ku-band imaging radar. For the tracking campaign of CanX-2 TIRA provided ranging, Doppler and angular measurements with a data rate of  $\sim 1.5$  Hz [9].

TIRA's location at  $50.6^\circ$  northern latitude and the sun-synchronous dusk-dawn orbit of CanX-2 lead to a regular visibility pattern of 2 to 3 station passes in the morning and evening of each day. Operation time constraints were incorporated into radar tracking planning. Out of the morning group of station passes the two passes with the highest elevation were selected for radar tracking, as well as 1 or 2 station passes in the evening of every second day. This observation schedule resulted in a total of 14 station passes to be tracked as illustrated in Fig. 2.

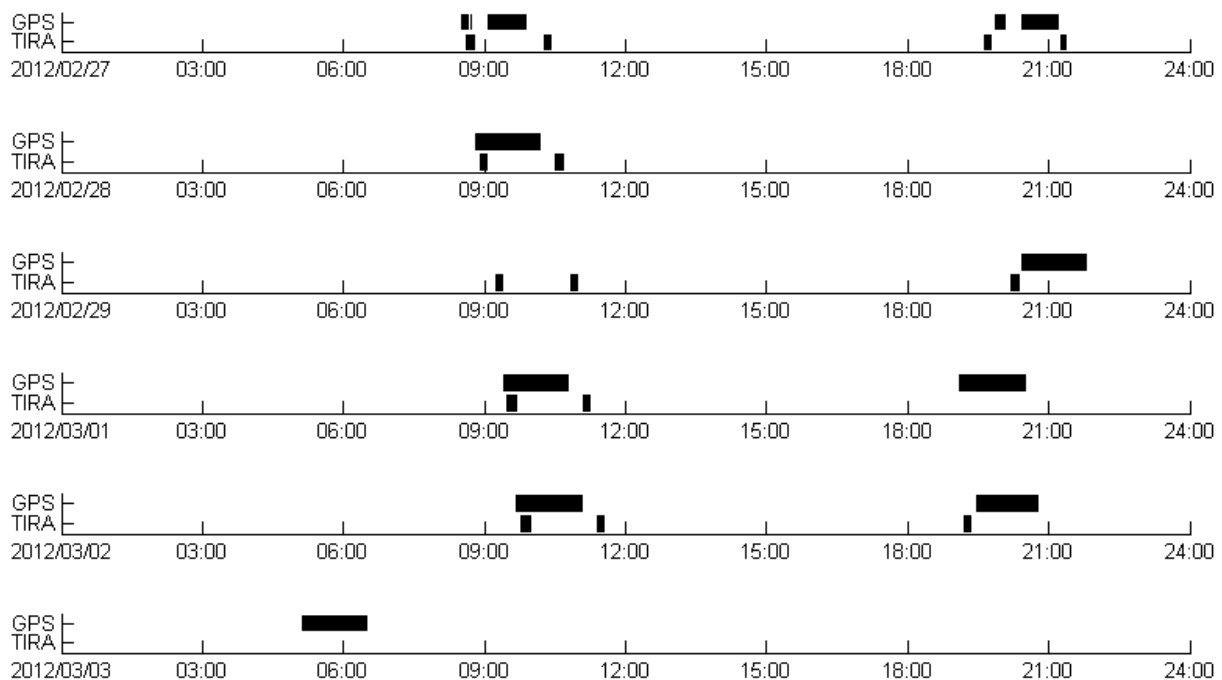


**Figure 2. Timeline of the Radar Tracking and GPS Operations**

TIRA successfully detected and tracked CanX-2 on each planned station pass. Of course, the maximum elevation varies from pass to pass, with the highest maximum elevation of  $85.9^\circ$  and lowest maximum elevation of  $13.2^\circ$ , both in the morning of March 02. Acquisition and loss of signal mainly occurred at very low elevations around  $5^\circ$ . Sometimes tracking acquisition took a while longer, accompanied by higher elevation of the first observation data from these passes. The performed radar tracking can still be described as horizon-to-horizon with uninterrupted measurements from the first to the last observation.

The timeline of GPS receiver operation is also shown in Fig 2. Two blocks of GPS measurements intended to be taken in the evening of February 28 and in the morning of February 29 are missing. The GPS data collection lasted one day longer than the radar tracking campaign which allows an assessment of the orbit determination accuracy over a certain propagation time.

### 3. Precise Orbit Determination from GPS Measurements

The precise orbit generated with CanX-2's GPS data is used as a reference for the radar measurement results. CanX-2 carries a NovAtel OEM4-G2L dual frequency GPS receiver, which provides L1 C/A tracking and semi-codeless L2 P(Y) tracking. Beside GPS navigation fixes the receiver delivers raw pseudorange and carrier phase measurements. To allow for precise orbit determination on ground the GPS raw observations are part of the downlink telemetry alongside the nanosatellite's attitude information.

A precise orbit was determined with the Reduced Dynamics Orbit Determination (RDOD) Software using GPS pseudorange and carrier phase measurements as input. The software was developed by the GNSS group at the German Space Operations Centre (GSOC) as part of the GPS High Precision Orbit Determination Software Tools (GHOST) [12]. The least squares residuals, given in Fig. 3, are a measure for how well the computed orbit fits the GPS measurements. The indicated accuracy of the estimated orbit is at the meter level for times of GPS operation. A long data gap exists from Feb. 28, 10:10 UTC to Feb. 29, 20:27 UTC. To quantify the degradation of orbit determination (OD) during the gap a similar analysis was made with TerraSAR-X precise orbit determination.

TerraSAR-X is equipped with a single frequency MosaicGNSS receiver and a dual frequency Integrated Geodetic and Occultation Receiver (IGOR). The most precise OD product, the science orbit, is computed with continuous raw observations from the IGOR receiver with estimated position accuracy below 10 cm [9].

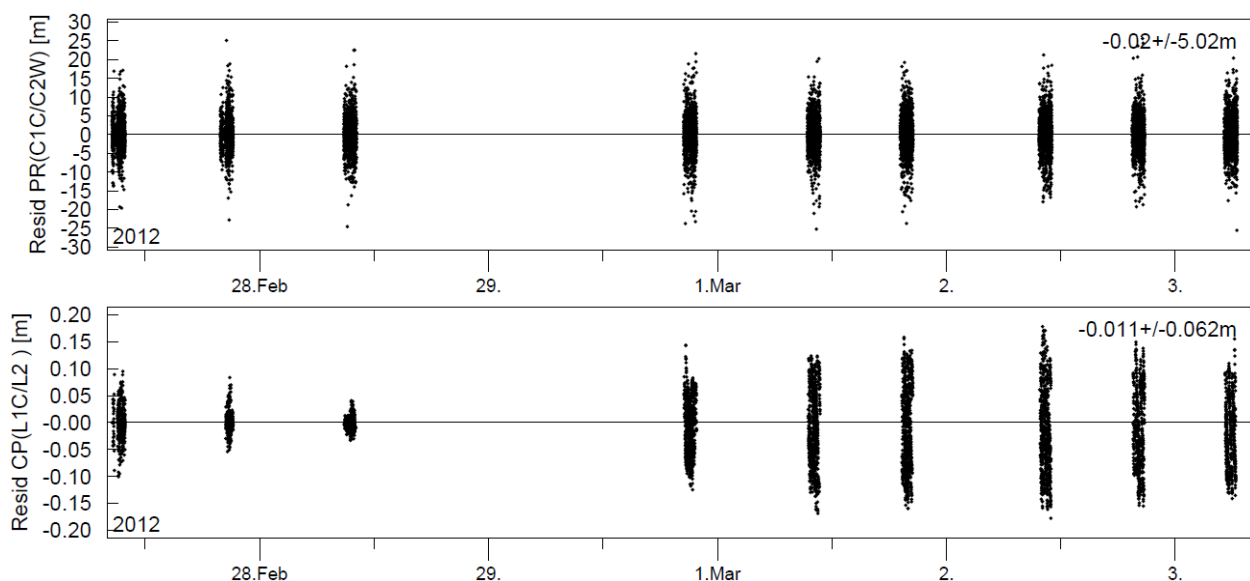


**Figure 3. GPS observation residuals after RDOD**

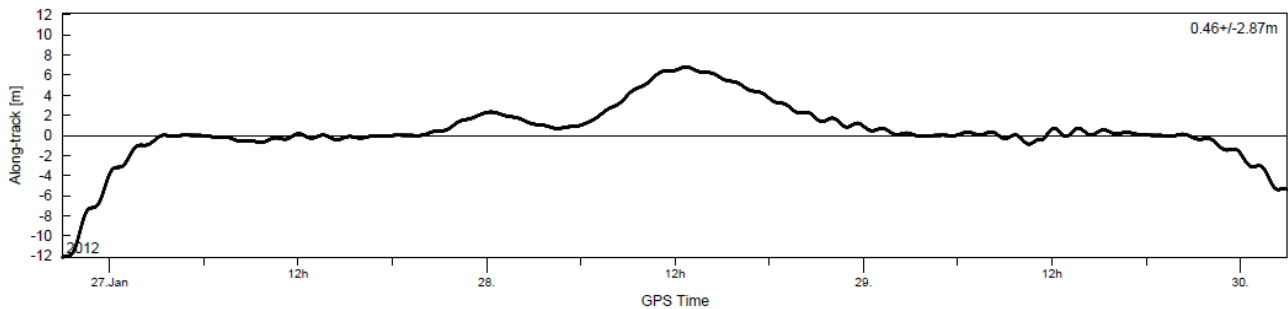


**Figure 4. TerraSAR-X along-track error due to similar GPS data gaps**

A subset of GPS data from TerraSAR-X is created adopting the CanX-2 receiver on-times from the measurement campaign. The edited dataset contains comparable GPS outages and is processed in the identical way using the RDOD software. The position solution computed from two IGOR measurement blocks before and after a long data gap of 34 hours is compared against the science orbit. The position error in the radial and cross-track directions stays below 1 m during the entire observation arc. This is not the case for the along-track component, which has a maximum deviation from the science orbit of around 8 m at the centre of the simulated large data gap, see Fig 4. The along-track error quickly rises outside the observation arc.

To summarize the findings of the similarity analysis, the length of a data gap is a critical parameter for the growth of position error primarily in the along-track component. For the example of the TerraSAR-X orbit, precision degrades by less than 1 m for short GPS data gaps of 12 hours and less than 10 m for GPS outages of 36 hours.

Multiday observation arcs may further deteriorate the OD solution, especially during long measurement gaps. A comparison of RDOD solutions obtained from CanX-2 GPS measurements of different observation arc lengths is an area for future work. As a consequence, the reference orbit is established from the full arc solution but relies on a 2 day short arc solution during the long data gap.

The estimated reference orbit accuracy is 1 m each for the radial and cross-track components and 5 m for the along-track component. During the GPS outage on the 28th and 29th of February orbit precision is difficult to estimate. Still, reference position information with meter level accuracy is well suited for the following radar tracking assessment.

#### **4 Calibration of the TIRA Tracking Radar**

CanX-2 is a triple CubeSat of the size 10cm x 10cm x 34cm [8]. Due to the non-spherical shape its radar cross section (RCS) becomes dependent on the aspect angle w.r.t. the radar, i.e its RCS will fluctuate during the measurements. For successful radar tracking of such small objects with the TIRA tracking radar [1] proper choice of the radar transmit power and acquisition threshold is necessary. The transmit power is set to a value such that the received echo power never exceeds the specified maximum input power of the receiver's low noise amplifier (LNA) under the assumption that the object reaches its maximum RCS. In the case of CanX-2 the expected echo power will stay far below the allowed value for all relevant passes, hence the radar transmitter can be operated with its maximum available output power.

The acquisition threshold is determined by the objects minimum RCS and lies above the radar's detection threshold. Its suitable adjustment minimizes the risk that unwanted, smaller objects which are also crossing the radar beam may disturb the target acquisition and the tracking phase or even cause a switch-over of the tracking loops to a false target.

As a preparatory step for setting this threshold an absolute calibration is conducted by tracking a spherical object with a well-known and constant RCS. Within the CanX-2 measurement campaign the calibration sphere TEMPSAT 1 was used having a RCS of -9.14 dBsm w.r.t. a radar transmit wavelength  $\lambda = 22.5$  cm. After computing the mean measured RCS around the closest point of approach (CPA) where the signal-to-noise ratio reaches its maximum, the RCS calibration factor is calculated as follows:

$$k_{RCS,cal} = RCS_{true} - \overline{RCS}_{meas} \quad [dB] \quad (1)$$

To obtain at least a coarse estimate of the minimum expectable RCS within a pass of CanX-2 we take into account its cuboid shape and assume that the RCS becomes minimal when the front edge of CanX-2 is oriented towards the radar so that edge-scattering becomes the prevailing contributor to the RCS. A pure corner-scattering is excluded here as the probability of its occurrence over a longer time period is considered to be low, and sporadic receive echoes with low amplitude are omitted by the radar processor. Now, the RCS approximation for a straight plate edge of length L [10]

$$RCS_{min} \approx RCS_{edge} \approx \frac{L^2}{\pi} \quad (2)$$

can be applied, resulting in a minimum RCS of -14:3 dBsm for  $L = 0.34$  m (long edge of CanX-2). In connection with Eq. (1) we finally get the acquisition threshold

$$RCS_{thres,TIRA} = RCS_{min} - k_{RCS,cal} \cdot \quad (3)$$

Involving  $k_{RCS,cal} = -7.5$  dB from the calibration measurements, Eq. (3) provides a threshold value of -6.8 dBsm.

## 5. Performance of the Radar Tracking Campaign

During the campaign all of the 14 planned tracking measurements could be realized and provided usable observation data. With the exception of one pass the acquisition of CanX-2 always succeeded for an antenna elevation  $Ele_{Ant} > 5^\circ$  which is higher than the nominal start value  $Ele_{Ant,min} > 1.5^\circ$  for TIRA. This increased acquisition elevation is mainly caused by the low RCS of CanX-2 in combination with refraction effects at low elevations.

The first acquisition attempt within the second pass of CanX-2 on Feb 27<sup>th</sup>, 2012 required a more detailed analysis: At the predicted rise time an object was acquired and tracked for several seconds that did not match CanX-2 (a later re-acquisition attempt at higher antenna elevation was successful). This case was caused by the presence of additional objects exceeding the threshold within the radar's field of view, a situation which typically occurs for example in the Launch and Early Orbit Phase of a mission shortly after the separation of the payload(s) from the upper rocket stage. Since CanX-2 was part of a multi-payload launch comprising ten satellites an orbit analysis of these objects indicates that the orbit of the Indian Cartosat 2A satellite had a minimum separation from CanX-2 in range and angle within the acquisition window.

Fig. 5 illustrates this angular separation  $\Delta\Phi$  which is approximately calculated from the antenna pointing (Azimuth, Elevation) for both objects based on the mean orbital parameters taken from their TLE:

$$\Delta\Phi(t) \approx \sqrt{(\Delta Azi(t)_{obj1-obj2} \cos(El e(t)_{obj1}))^2 + \Delta El e(t)_{obj1-obj2}^2} \quad (4)$$

It is clearly to be seen in Fig. 5 that, assuming CanX-2 is within the main lobe of the TIRA's antenna pattern, Cartosat 2A will indeed stay outside the main lobe but will cross the first side lobe at the beginning of acquisition ( $t < 25$  s).

The attenuation of the first side lobe of TIRA's antenna pattern is about 17.5 dB [11] w.r.t. the main lobe which is sufficiently high for most of TIRA's tracking tasks. But Cartosat 2A with an estimated RCS of +7 dBsm, i.e. more than 20 dB higher than the RCS of CanX-2 computed according to Eq. 2, induces a side lobe receive power considerably above the receive power of CanX-2 in the main lobe. This triggers the so-called side lobe tracking which continues until the track is lost due to the growing differences between the predicted and measured angular positions. Side lobe tracking can't be avoided in principle when using one single receive antenna as it is impossible to distinguish between a "strong" target in the side lobe and a "weak" target in the antenna's main lobe. Currently, this problem can only be handled by manual intervention of the radar operator.

A first assessment of the collected radar measurements is a simple comparison of radar positions against the GPS reference orbit. Range and elevation measurements are therefore corrected for tropospheric refraction using the Hopfield troposphere model. The deviation of all range, azimuth and elevation measurements gathered on a representative station pass is plotted in Fig. 6, alongside the received signal amplitude. It can be seen that the range outliers are few and are time-correlated with a low signal to noise level. The range measurements contain outliers of up to 10 km on 6 of the total 14 station passes. Doppler measurements are largely biased on all radar passes. For times of stable object tracking the estimated 1- $\sigma$  single measurement point accuracy is  $\sim 10$  m in range,  $\sim 100''$  for angular observations and  $\sim 200$  cm/s for Doppler measurements.

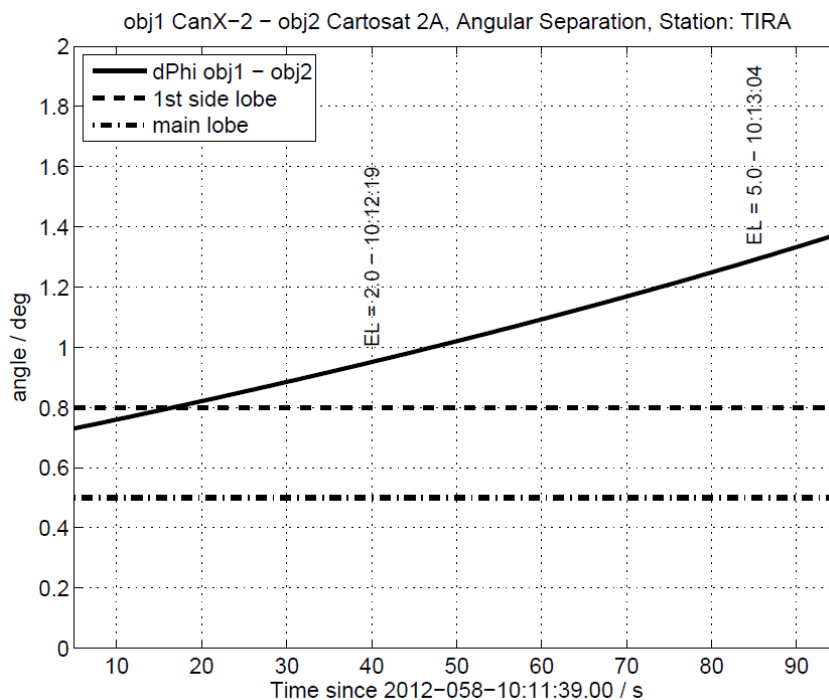


**Figure 5. Angular separation of CanX-2 and Cartosat 2A during the acquisition phase**

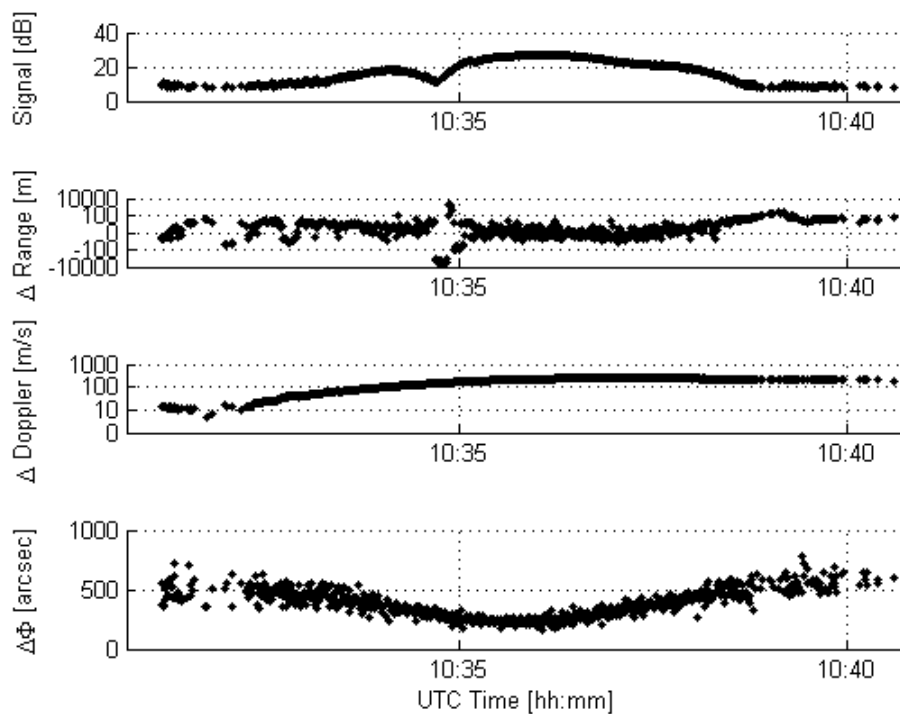


**Figure 6. TIRA measurements from the second station pass of February 28**

## 6. Orbit Determination from Radar Tracking Data

The orbit determination software ODEM (Orbit Determination for Extended Maneuvers) is used to generate a batch least squares fit solution for all OD cases. Initial position and velocity values are found from interpolation of the GPS reference orbit. Single measurement points with significant deviations from the initial orbit in the first OD iteration step, or from the improved orbit in subsequent iteration steps, are excluded from the OD computation. For this purpose, the measurement editing level can be set in ODEM. To deal with outliers in the process of orbit determination, a large editing level is set in the first iteration step when rough state estimates are available, and a more restrictive editing level is set in all following iteration steps when OD has already converged to the final solution. The following software settings are used:

- dynamic modeling
  - spherical harmonic geopotential of order and degree 60
  - third body attraction by sun and moon
  - solar radiation pressure, atmospheric drag
- measurement noise
  - 10 m in range, 100'' for azimuth and elevation
- measurement editing level
  - 10000 times the measurement noise for initial step,
  - 5 times the measurement noise for subsequent steps
- maximum number of iterations
  - 15
- additional estimation parameters
  - drag coefficient, constant measurement bias
- ephemeris generation
  - first obs. to last obs.+ 72 h, 30 s sampling interval

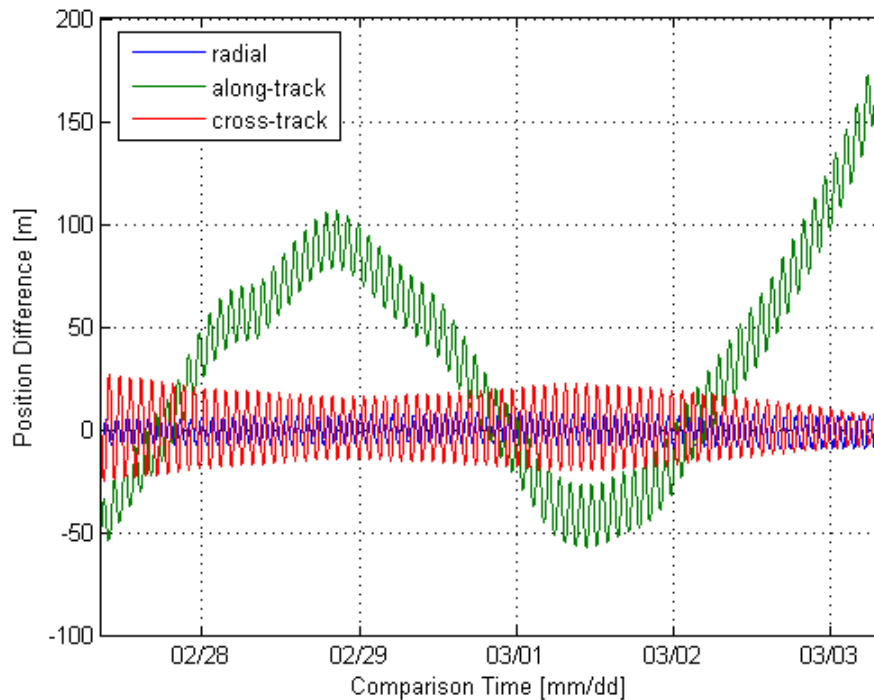


**Figure 7. Operational OD from all TIRA observation data vs. GPS reference orbit**

The position differences between an OD solution incorporating all radar tracking data and the GPS reference orbit is shown in Fig. 7. In general, the position deviations are approximately 1 to 2 orders of magnitude larger than the estimated accuracy of the GPS reference orbit.

The along-track component shows a characteristic curve shape. One reason is probably the different orbit models applied in the ODEM and RDOD software. Unlike GPS processing, which is based on a reduced dynamic orbital motion model with empirical accelerations estimation every 8 hours, a purely dynamic motion model is applied in ODEM. Alongside the state vector a constant atmospheric drag coefficient and a constant solar radiation pressure coefficient are additionally estimated. Effectively, less flexibility is given to the orbital model to adjust to an observation arc spanning several days. Since the typical radar tracking duration for collision avoidance support does not exceed 24 h [1] and the following OD analysis will focus on observations arcs of up to 48 h, these concerns are not taken into account.

Processing both observation data within the same OD software and with identical orbital model will reveal the additional error introduced by varying OD processes and is subject to future work.

## 5. Statistical Analysis Methodology

Out of all tracking data provided by FHR smaller data sets are selected to construct tracking scenarios for collision avoidance support. Normally, less than 48 hours are left to collect observations and compute refined orbital information of the secondary object. For a single sensor, the number of available station passes typically ranges from 5-10 within 48 hours. Based on the full data set of 14 station passes multiple cases with comparable tracking duration and identical number of station passes can be selected. Beyond comparing single orbit determination (OD) cases with the reference orbit it is therefore possible to derive statistical quantities on the achievable orbit determination accuracy. Mean position errors are computed for the time of the observation arc and for propagation times of up to 72 hours. The obtained error statistics may be used to improve tracking planning effectiveness and secure realistic collision risk assessment.

**Table 1. Number of OD cases for different tracking scenarios, “M xor E” indicated by \*.**

	0 h*	12 h	24 h*	24 h	36 h	48 h*	48 h
2 passes	6	14	16	0	10	15	0
3 passes	0	11	16	12	27	37	28
4 passes	0	2	4	16	25	39	74
5 passes	0	0	0	7	9	18	82
6 passes	0	0	0	1	1	3	44
7 passes	0	0	0	0	0	0	11
8 passes	0	0	0	0	0	0	1

The selection of 2-8 station passes from the full data set results in a total number of 529 orbit determination cases with a principal tracking duration of 48 h. The term principle tracking durations reflects the presence of two groups of station passes every day for polar orbiting satellites. The principle tracking duration is always a multiple of 12 hours as the groups of station passes on the ascending and descending arc are separated by half of the Earth rotation time. The real tracking duration may last up to 6 hours longer or shorter than the value of the principle tracking duration.

No case could be constructed with more than 8 station passes within 48 hours. Statistical analysis is performed over groups of comparable OD cases and therefore for various OD scenarios. The scenarios differ in the principal tracking duration. The station passes on the ascending and descending orbital arcs are combined (combination of morning and evening passes for sun-dusk orbit respectively). For OD cases having a principal tracking duration of 0 h, meaning all observations are taken on station passes from subsequent orbits, only morning passes or evening passes are involved. By definition an arbitrary selection of station passes within a principal tracking duration of 12 h and 36 h will always be a combination of morning and evening passes. The 24 h and 48 h OD scenarios may be an exclusive combination of morning or evening passes, or may be a mixture of passes at both times of day. The two types of combinations are analyzed separately for the 24 h and 48 h scenarios. Mixed combinations are labeled “M and E” and scenarios that are exclusively based on morning or evening passes are labeled “M xor E”.

The number OD cases per OD scenario group is given in Tab. 1. Large variations in the statistical basis can be seen among the scenarios. A larger number of combinations exist for longer tracking durations and a balanced ratio of passes that are included and excluded from a specific OD case. The last station pass of each OD case defines the maximum time the propagated OD solution can be compared against GPS reference orbit that ends at 2012/03/03 08:00 UTC. The total numbers of OD cases that can be evaluated after various propagation times are listed in Tab. 2.

**Table 2. Number of evaluable OD cases for different propagation times**

Time Interval	Observation	24h Propagation	48h Propagation	72h Propagation
# OD Cases	529	404	310	57

## 6. Analysis Results

A convergent solution is obtained in all 529 cases of orbit determination from radar tracking data. Sometimes, a significant number of measurement points are rejected because of range outliers. 29 OD cases have therefore been reprocessed with a higher editing level in the second iteration step. Comparison with the GPS reference orbit confirmed lower position errors.

For all OD cases of the same tracking scenario a mean value of the root mean square errors during observation arc is computed. The radial, along-track and cross-track components of these mean position errors are depicted in Fig. 8. The largest position error is always attributable to the along-



All OD solutions from advantageous combinations of morning and evening passes are propagated in time. The mean position errors after 24 h, 48 h, and 72 h are plotted in Fig. 10 – 12. For comparison, Fig. 9 holds the mean position errors for the observation arc with the same scaling of the error axis. The growth of position error which does not linearly depend on propagation time can clearly be seen. Errors have barely grown 24 hours after the last observation. They increasingly rise after 48 hours and rise more severely after 72 hours. Moreover, orbit precision clearly depends on the principal tracking duration. Long time intervals between the first and last observation allow precise drag coefficient estimation and therefore more robust and accurate orbit propagation.

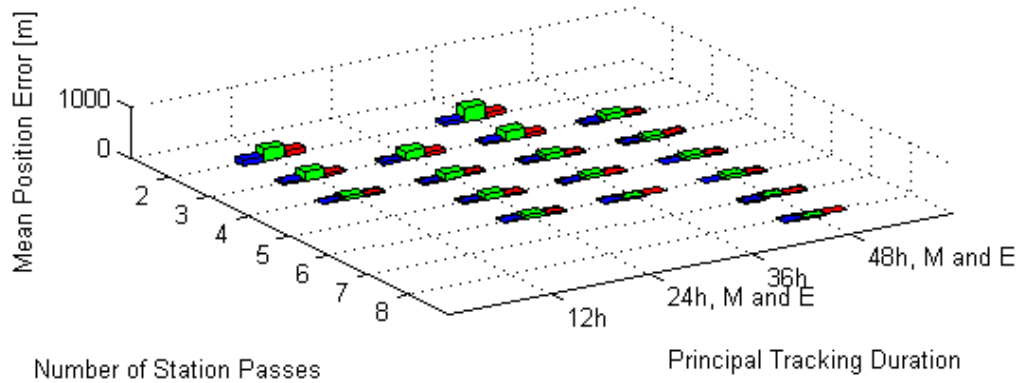


**Figure 9: Mean position errors for observation arc.**

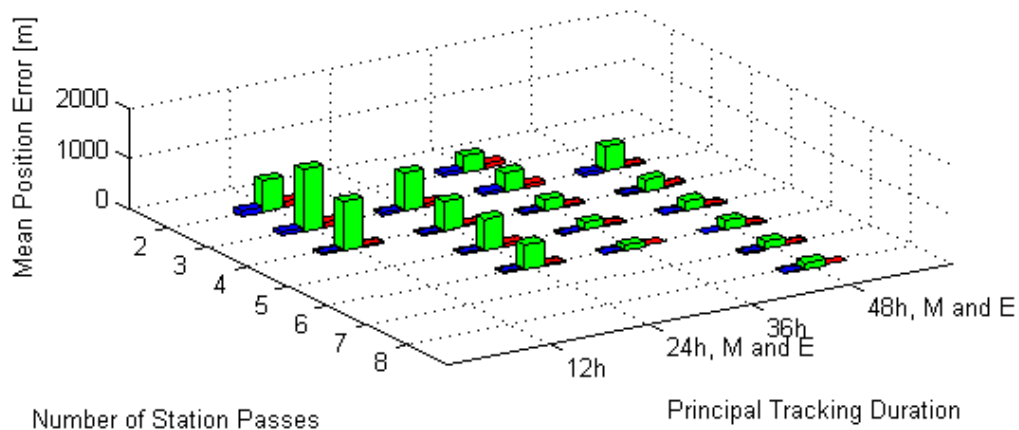


**Figure 10: Mean position errors after 24 hours propagation.**

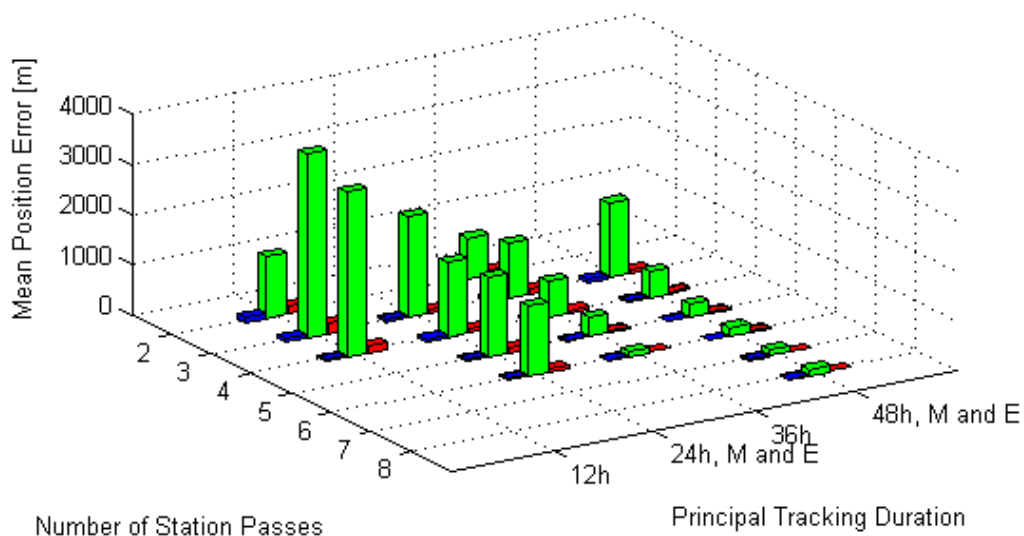


**Figure 11: Mean position errors after 48 hours propagation.**

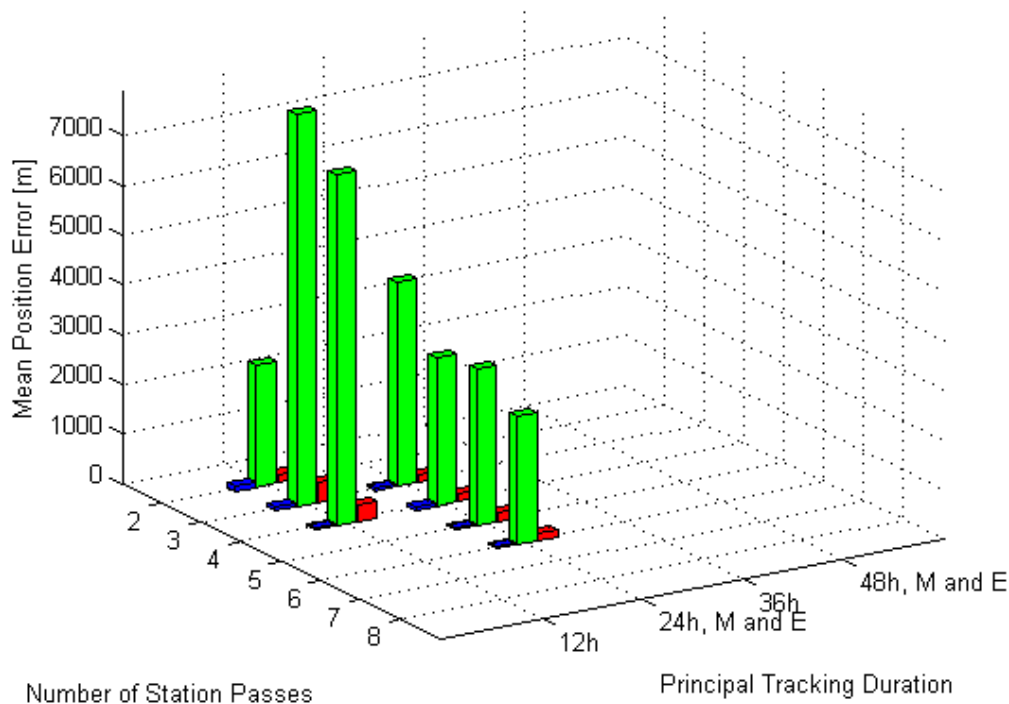


**Figure 12: Mean position errors after 72 hours propagation.**

## 7. Conclusions

In the course of a 5 day long tracking campaign observation data on the nanosatellite CanX-2 were successfully gathered by the on-board GPS receiver as well as the Tracking and Imaging Radar of FHR. An appropriate reference orbit was computed from the GPS raw measurements. TIRA proved to be a suitable sensor for providing positional information on a man-made object in LEO of cm-size. Meaningful statistics on the orbit precision were derived for different radar tracking scenarios.

The radial position error of a small debris-like object stays below 40 m for a propagation time of 24 hours, a representative time interval between the end of the radar tracking and a predicted collision event. A significant orbit refinement can be achieved compared to the usual TLE accuracy. Radar tracking for collision avoidance support is therefore a useful tool to mitigate space debris collision risks and reduce the number of avoidance maneuvers.

The following lessons have been learned for the planning of radar tracking campaigns to support collision risk assessment by refined orbit determination.

- Tracking scenarios comprising of a single group of station passes from the same ascending or descending orbital arc only, e.g. 2 radar passes from subsequent orbits, result in position errors larger than 1 km during the observation arc and even worse for orbit propagation.
- The principal tracking duration for collision avoidance support should be at least 12 h and preferably longer. This conflicts with the typical collision avoidance timeline. Longer observation arcs can only be achieved with an early decision for radar tracking. This is connected to a lower prediction confidence and subsequently to more frequent tracking requests.
- Tracking scenarios with a principal tracking duration of 24 h or 48 h should be a mixed combinations of station passes from the ascending and descending orbital arc. Mixed

combinations imply observations are taken from opposite sites of the orbit. The more diverse tracking geometry facilitates a better OD accuracy.

- The orbit precision deteriorates with increasing propagation times. There is a moderate accuracy within the first 24 h after radar tracking. This relaxes conflicts with the time before closest approach required for maneuver planning and execution. Again longer observation arcs are preferred to gain prediction stability.

The orbit precision results are valid for other radar tracking applications, such as orbit determination for On-Orbit Servicing and Active Debris Removal.

The analysis was carried out for a single satellite and during relative calm solar activity. The solar 10.7 cm flux increased from ~100 sfu at the beginning of tracking campaign to ~120 sfu at the campaign end. Orbit prediction errors strongly depend on atmospheric drag and therefore on orbital height and solar activity. Similar tracking campaigns and analysis should be re-performed for a number of satellites within different orbital altitudes and in times of high solar activity.

Future work will focus on a more detailed measurement data evaluation from the CanX-2 tracking campaign. Further aspects of the orbit determination process will be analyzed. As mentioned, the impact of different orbital models should be assessed. Next, orbit precision can be expressed in terms of errors in keplerian elements. And it would be interesting to compare the covariance information computed during orbit determination and propagated in time against the real position errors.

## 8. References

- [1] S. Aida, T. Patzelt, L. Leushacke, M. Kirschner, and R. Kiehling, "Monitoring and Mitigation of Close Proximities in Low Earth Orbit", 21<sup>st</sup> ISSFD Conference, Toulouse, France, 2009.
- [2] S. Aida, M. Kirschner, M. Wermuth and R. Kiehling, "Collision Avoidance Operations for LEO Satellites Controlled by GSOC", SpaceOps Conference, Huntsville, Alabama, 2010.
- [3] S. Aida and M. Kirschner, "Collision Risk Assessment and Operational Experiences for LEO Satellites at GSOC", 22<sup>st</sup> ISSFD Conference, São José dos Campos, Brazil, 2011.
- [4] S. Aida and M. Kirschner, "Operational Results of Conjunction Assessment and Mitigation at German Space Operations Center", 28<sup>th</sup> ISTS Conference, Okinawa, Japan, 2011.
- [5] Kahr, E. and Montenbruck, O. and O'Keefe, K. and Skone, S. and Urbanek, J. and Bradbury, L. und Fenton, Pat, F., "GPS Tracking of a Nanosatellite – The CanX-2 Flight Experience", 8th International ESA Conference on Guidance, Navigation & Control Systems, 5.-10. June 2011, Karlsbad, CZ.
- [6] Thakker P. and Shiroma W. A.; "Emergence of Pico- and Nanosatellites for Atmospheric Research and Technology Testing"; AIAA Progress in Astronautics and Aeronautics Series, vol. 234; American Institute of Aeronautics and Astronautics, 2010.
- [7] Sarda K., Eagleson S., Caillibot E. P., Grant C., Kekez D. D., Pranajaya F. and Zee R. E.; "Canadian Advanced Nanospace Experiment 2: Scientific and Technological Innovation on a Three-Kilogram Satellite", *Acta Astronautica*. 59:236-245, 2006.

- [8] K. Sarda et al, "Canadian Advanced Nanospace Experiment 2 Orbit Operations: One Year of Pushing the Nanosatellite Performance Envelope", 23rd Annual AIAA/USU Conference on Small Satellites (Logan, Utah, USA), 2009.
- [9] Wermuth, M. and Hauschild, A. and Montenbruck, O. and Jäggi, A., "TerraSAR-X Rapid and Precise Orbit Determination", 21st International Symposium on Space Flight Dynamics, , Toulouse, France, 28 Sept.- 2 Oct. 2009.
- [10] M. I. Skolnik, Radar Handbook, McGraw-Hill, New York, 1990.
- [11] D. Mehrholz, „Radardatengewinnung und Fehleruebertragung bei der Beobachtung von nichtkooperativen Objekten im erdnahen Weltraum“, Ph.D. thesis, Universitaet der Bundeswehr Muenchen, Dec. 1988.
- [12] Montenbruck O., van Helleputte T., Kroes R. and Gill E.; "Reduced Dynamic Orbit Determination using GPS Code and Carrier Measurements"; Aerospace Science and Technology 9/3, 261-271 (2005). DOI 10.1016/j.ast.2005.01.003.